

## Polyamide-6/Boron Nitride 열전도성 복합재료의 모폴로지 및 열적 특성과 결정화 거동

Ru Xia<sup>†</sup>, Manman Sun, Bin Yang<sup>†</sup>, Jiasheng Qian, Peng Chen, Ming Cao, Jibin Miao, and Lifan Su

College of Chemistry & Chemical Engineering,  
Key Laboratory of Environment-Friendly Polymeric Materials of Anhui Province, Anhui University  
(2017년 7월 28일 접수, 2017년 9월 15일 수정, 2017년 9월 17일 채택)

### Morphology, Thermal and Crystallization Properties of Polyamide-6/Boron Nitride (BN) Thermal Conductive Composites

Ru Xia<sup>†</sup>, Manman Sun, Bin Yang<sup>†</sup>, Jiasheng Qian, Peng Chen, Ming Cao, Jibin Miao, and Lifan Su

College of Chemistry & Chemical Engineering, Key Laboratory of Environment-Friendly Polymeric Materials of Anhui Province, Anhui University, Hefei 230601, Anhui, P. R. China

(Received July 28, 2017; Revised September 15, 2017; Accepted September 17, 2017)

**Abstract:** A series of the thermal conductive polyamide-6 (PA6) composites filled with boron nitride (BN) were prepared by two methods, including melting method (MM) and solution method (SM). The thermal conductivity, morphology, crystallization behavior, thermal stability, and rheological properties of PA6 composites were investigated. The results showed that the thermal conductivity of two methods increased with increase in the filler content, the thermal conductivity of PA6/BN composites containing 40 wt% BN prepared by melting method was up to  $1.02 \text{ W}\cdot\text{m}^{-1}\cdot\text{K}^{-1}$ , while the thermal conductivity of PA6/BN composites prepared by solution method was up to  $1.44 \text{ W}\cdot\text{m}^{-1}\cdot\text{K}^{-1}$  at the same filler content.

**Keywords:** polyamide-6, boron nitride, melting method, solution method, thermal conductivity.

## Introduction

With the development of electronic packaging technology, the electronic devices tend to bear ultra-thin, lightweight and multifunctional properties. Large amounts of heat generated or accumulated in the electronic devices should be dissipated quickly in order to prolong the service life of electronic products.<sup>1-3</sup> Generally, common polymers have relatively low thermal conductivity (typically only  $0.2 \text{ W}\cdot\text{m}^{-1}\cdot\text{K}^{-1}$ ),<sup>4</sup> which are not suitable for thermal materials application. The incorporation of highly thermal conductive fillers into polymers to develop high-performance thermal-conductive composites had been mostly desired so far.<sup>5</sup> The composites based on crystalline polymers (e.g., polypropylene,<sup>6</sup> polyamide-6,<sup>7,8</sup>) provided enhanced thermal conductivity as compared to those based on amorphous polymers. And the thermal conductivities of com-

posites were highly enhanced by using various thermal conductive fillers, such as, graphites, graphene, carbon nanotubes (CNTs), carbon fibers (CFs) and boron nitride (BN).<sup>9</sup>

Many articles have been published on improving the thermal conductivity of polymer composites.<sup>10,11</sup> Besides, the direction of different preparation methods were also extensively investigated. Various approaches had been taken for the formation of the polymer composites: *in situ* polymerization, solution blending, powder blending, roller mixing and melt mixing, according to the different states of the process.<sup>12</sup> The different preparation methods would affect the dispersion, distribution, orientation and length to diameter ratio of the filler in the matrix,<sup>13</sup> and then influence the thermal conductivity of the composites. For example, Agari *et al.*<sup>14</sup> prepared PE/graphite composites by four methods, and the thermal conductivity became higher in the following order: melt mixture < roll-milled mixture  $\approx$  solution mixture < powder mixture. A majority of current researches have proved that the solution mixing effectively improved the dispersion of the filler in the polymer matrix, reduced aggregation which further improved the thermal conductivity.<sup>15-17</sup>

<sup>†</sup>To whom correspondence should be addressed.  
xiarucn@sina.com, ORCID<sup>®</sup> 0000-0002-4549-2964  
yangbin@ahu.edu.cn, ORCID<sup>®</sup> 0000-0003-1184-317X  
©2018 The Polymer Society of Korea. All rights reserved.

As a widely used engineering plastic, PA6 offered good thermal stability, chemical resistance and excellent mechanical properties.<sup>18</sup> And the conductive filler of hexagonal BN (h-BN) was a lamellar material with a graphite-like structure in which planar networks of BN hexagons were regularly stacked.<sup>19,20</sup> It has the highest thermal conductivity among ceramic materials and also an electronic insulator. In addition, bulky hexagonal BN can be exfoliated into mono- and/or few-layers of BNNs in various solvents thus obtained high aspect ratio.<sup>21-23</sup> Therefore, BN-filled polymer composites, especially the lamellar BN, not only inherit the insulating properties of the polymer matrix but also impart polymer composites thermal conductivity in comparison to conventional fillers, such as, Al<sub>2</sub>O<sub>3</sub>, ZnO, AlN, and SiC.<sup>24-26</sup>

Liu *et al.*<sup>15</sup> reported that the maximum value of thermal conductivity of carbon fiber/PA66 composites containing 40 wt% carbon fiber prepared by SM achieved 2.537 W·m<sup>-1</sup>·K<sup>-1</sup>, which was superior to carbon fiber/PA66 composites prepared by EM at the same filler content. Hong *et al.*<sup>27</sup> demonstrated that aluminum nitride (AlN) and boron nitride (BN) were found to be the ideal heat dissipation materials for thermal packaging after he investigated the properties of AlN/BN epoxy composites.

The aim of this paper was to investigate the preparation and thermally conductive, morphology and crystallization properties of polyamide composites based on BN filler. Two methods were used to prepare the PA6 composites which including melting method and solution method. The results will be discussed and provided theoretical bases for the preparation of composites with excellent thermal conductivity.

## Experimental

**Materials.** In this work, a commercial grade of PA6 (Model: UBE-1013B, product of UBE, Thailand) was adopted with a melt flow rate (MFR) of 13.9 g/10 min (under 275 °C/0.325 kg) and a melting temperature of 222 °C. h-BN powder, size approximately 5 μm, purchased from Dandong Rijin Technology Co. China, was used as the thermally conductive filler, whose density was 2.27 g/cm<sup>3</sup> and thermal conductivity 10-35 W·m<sup>-1</sup>·K<sup>-1</sup>. Other chemical additives and solvents were obtained commercially and were used as received.

**Preparation of Composites.** Prior to blending, both PA6 resin and h-BN filler were vacuum dried at 80 °C for 16 h and 80 °C for 8 h to remove residual moisture, respectively.

Thermal conductive PA6 composites were prepared by the

following two methods:

(1) Melting Method (MM): The PA6 resin, thermal conductive filler of h-BN and some antioxidants were proportionally mixed in a high-speed blender for 5 min and then processed in Haake torque rheometer (Thermo Hakke, Polylab OS, Germany) to prepare samples. Irganox 1010 and 168 were added as antioxidants into the mixture with a loading of 0.5 wt%. The rotational speed of torque was 60 r/min, the processing temperature and time were 230 °C and 10 min, respectively. The samples were dried at 80 °C for 16 h to remove moisture. According to this method, the PA6/BN composites with various filler mass fractions were prepared.

(2) Solution Method (SM): PA6 particles were completely solved in 88 wt% formic acid (HCOOH) water solution and stirred at 70 °C for 1 h. h-BN powders were dispersed in formic acid and ultrasonic for 5 h. Subsequently, the PA6 solution and h-BN solution were mixed together with 2 h of stirring. Then the mixture was condensed at 100 °C to remove the most part of solvent and poured into the glass mold, put the concentrated liquid into the oven, dried at 80 °C for 24 h. The residual formic acid was cleaned by ethanol and the samples were dried at 80 °C for constant weight. Finally, the PA6/BN composites with various filler mass fractions were prepared.

In order to differentiate and define each sample clearly, the following designation rules were applied. For each preparation method, BN added in by different mass ratio of the whole (PA6/BN) system. M10, M20, M30, M40 were used to indicate the composites prepared by melting method contained BN of 10, 20, 30, 40 wt%, respectively. S10, S20, S30, S40 were used to indicate the composites prepared by solution method contained BN of 10, 20, 30, 40 wt%, respectively. And the original sample was represented by neat PA6.

**Thermal Properties.** The thermal conductivity of samples were carried out by a Transient Plane Source Method (TCi-3-A, Canada) in an air-conditioned room (25 °C). The samples were cured and prepared in cylindrical shape of 25 mm in diameter and 2.0 mm in thickness, depending on the actual thermal conductivity. All of the thermal measurements were performed three times and the averages were taken to calculate the thermal conductivity.

**Scanning Electron Microscope.** The morphology of the composites was evaluated by a field-emission scanning electron microscopy (SEM, S-4800, Hitachi, Tokyo, Japan). Samples were cryogenically fractured in liquid nitrogen and all of the fractured surfaces were coated with gold to enhance the image resolution and to prevent electrostatic charging.

**Differential Scanning Calorimetry (DSC).** The melting and crystallization behaviors of PA6/BN composites were studied using a differential scanning calorimetry (DSC, Model: Q-1000, product of TA Instruments Inc.). During the measurement, each sample weighed ~5 mg was hermetically-sealed in the aluminum pans under nitrogen (N<sub>2</sub>) atmosphere. At first, sample was heated from 30 to 250 °C at 10 °C/min and kept at 250 °C for 5 min to eliminate the thermal history. Subsequently, the samples were cooled to 30 °C at a cooling rate of 10 °C/min and kept at 30 °C for 5 min, then samples were heated from 30 to 250 °C at 10 °C/min, respectively. Both first and second endothermic curves were recorded. Degree of crystalline ( $X_c$ ) was calculated from melting enthalpy values using the following equation:

$$X_c = \frac{\Delta H_m}{(1-\lambda)\Delta H_m^0} \times 100\% \quad (1)$$

where  $\Delta H_m$  is second melting enthalpy of the samples,  $\Delta H_m^0$  is the enthalpy value of melting of the 100% crystalline form of PA6 (188 J g<sup>-1</sup>),<sup>7</sup> and  $\lambda$  is the mass fraction of BN.

**Thermal Gravimetric (TG).** The thermal stability of the composites were studied by thermalgravimetric (LABSYS evo DTA/DSC 1150, Setaram Instruments Co.). Each sample was weighed about 5~10 mg and tested under nitrogen (N<sub>2</sub>) atmosphere. At first, sample was maintained at 40 °C for 10 min, and subsequently heated from 40 to 800 °C at 20 °C/min. Finally, the curves of the residual weight percentage of the sample *versus* the sample temperature were obtained.

**Rheological Measurement.** Viscoelastic behavior of the samples was analyzed in a dynamic rheometer (Bohlin Gemini 2000, Malvern Instruments Ltd., UK) in the melt state and the gap value was 1 mm. Tests were carried out within linear viscoelastic region for 260 °C in a frequency sweep range from 0.01 to 100 Hz. Furthermore, to ensure that the rheological properties were measured in linear viscoelastic region, the strain range was prior determined from strain sweeps. All the measurements were conducted in the strain range of 1%, and under nitrogen (N<sub>2</sub>) atmosphere to avoid the oxidative degradation of samples.

**X-ray Diffraction (XRD).** X-ray diffraction was performed using a SmartLab Analytical X-ray (Model: SmartLab 9 kW, Rigaku Corporation, Japan) with area detector operating under 40 kV and 100 mA of CuK $\alpha$  radiation ( $\lambda=0.1542$  nm). And the XRD patterns were recorded with a scan rate of 20°/min from  $2\theta=5^\circ$  to  $90^\circ$ .

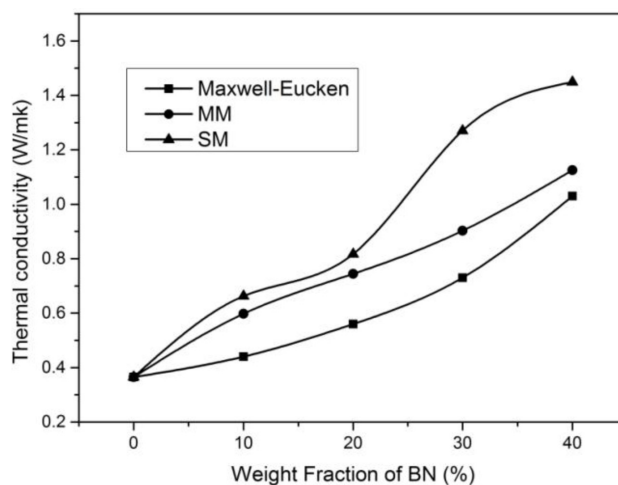


**Figure 1.** Comparison of experimental and theoretically predicted thermal conductivity of PA6/BN composites.

## Results and Discussion

**Thermal Properties.** The effects of filler addition and processing methods on thermal conductivity of PA6/BN composites showed in Figure 1. The thermal conductivity of two methods were both increasing with the loading of BN, the thermal conductivity of composites prepared by melting method was up to  $1.02 \text{ W}\cdot\text{m}^{-1}\cdot\text{K}^{-1}$  containing 40 wt% BN fillers, while the thermal conductivity of composites prepared by solution method was up to  $1.44 \text{ W}\cdot\text{m}^{-1}\cdot\text{K}^{-1}$  at the same filler content, revealed a 2.8-fold and 3.9-fold gain compared to neat PA6 with thermal conductivity value of  $0.36 \text{ W}\cdot\text{m}^{-1}\cdot\text{K}^{-1}$ .

It was obviously seen that the thermal conductivity of composites prepared by SM was superior than MM, which was consistent with the results of T. Liu and Q. Mu.<sup>15,16</sup> This is attributed to simple blending to form a large agglomerate of fillers during mixing resulting in their poor dispersion and further influence the conductive network of polymer composites. However, the solution mixing of each component in a co-solvent brings about a good molecular level of mixing overcoming the agglomeration tendency of the conductive fillers. It is applicable to the polymers which can be dissolved or swelled by the solvent.<sup>28</sup> In terms of single preparation method, the study of Lee showed that the thermal conductivity of the composites increased with the addition of conductive filler. while in low filling condition, the thermal conductivity increased slowly and the thermal conductivity of the composites increased obviously when the filling amount reached a certain value which revealed the formation of conductive network between

matrix and filler. In this paper, the results of SM were consistent with the study of Lee.<sup>29</sup>

Different preparation methods would affect the filler dispersion and compatibility, which finally lead to the microstructure difference.<sup>30</sup> In this study, the MM mixed PA6 and BN by using a Haake mixer at 230 °C and 60 rpm/min. The SM mixed PA6 and BN in solvent environment and the BN were pre-exfoliated in formic acid via ultrasonication before mixing with the PA6 matrix. As is well known, traditional processes, such as simple blending by a two-roll mill or internal mixer, are hardly sufficient to uniformly disperse BN particles and always lead to the severe aggregation of BN in the polymer matrix, thus resulting in low thermal conductivity.<sup>26,28</sup>

Maxwell-Eucken model was used to evaluate the thermal conductivity of polymer composites which the thermal conductive fillers were homogeneous sphere with no interaction and dispersed randomly in the polymer matrix.<sup>31</sup> It could predict the thermal conductivity of polymer composites precisely at the low filler content. Mathematical expression of the Maxwell-Eucken model:

$$\lambda = \lambda_1 \left[ \frac{2\lambda_1 + \lambda_2 + 2v(\lambda_2 - \lambda_1)}{2\lambda_1 + \lambda_2 - 2v(\lambda_2 - \lambda_1)} \right] \quad (2)$$

where  $\lambda_1$ ,  $\lambda_2$ , and  $\lambda$  were the thermal conductivity of polymer matrix, filler, and polymer composites, respectively. Where  $v$  was the volume fraction of filler particles. While at the high filler, it had a big difference between the theoretical prediction and the experimental data, which because the formation of conductive network between matrix and filler, when the filling amount reached a certain value. The Maxwell-Eucken model would not apply to evaluate the thermal conductivity of polymer composites.

In this study, Maxwell-Eucken model was used to predict the thermal conductivity of PA6 composites. From Figure 1, it was showed that the experimental data did not agree well with the Maxwell-Eucken model, and the experimental data were always higher than the predicted ones. Because the model assumed that the filler shape is sphere and confined to common dispersion state in the polymer matrix. However, the h-BN had lamellated structure and the special dispersion state of filler formed here obviously exceeded the predicted limits of the model, which finally led to an improvement on the thermal conductivity of PA6/BN composites.

Agari model introduced the parallel and vertical conduction mechanism,<sup>14</sup> this model is suitable for uniform distribution of layered fillers, on the basis of previous studies. It can be used

**Table 1.  $C_1$  and  $C_2$  of Agari Model for PA6/BN Composites with Different Methods**

Preparation method	$C_1$	$C_2$
MM	1.43	0.69
SM	1.56	0.95

to investigate the effect of dispersion state by introducing two factors  $C_1$  and  $C_2$ :

$$\log \lambda = vC_2 \log \lambda_2 + (1-v) \log (\lambda_1 C_1) \quad (3)$$

where  $C_1$  is a factor relating to the structure of polymer, such as crystallinity of matrix, and  $C_2$  is a factor relating to the measure of ease for the formation of conductive chains of filler. According to Agari model, the closer the  $C_2$  values are to 1, the more easily conductive chains are formed in composites. After a calculation, the value of  $C_1$  and  $C_2$  were obtained as listed in Table 1.

It can be observed from Table 1 that the value of  $C_2$  in PA6/BN composites prepared by SM was very close to 1, which indicated it was more easily to form the conductive chains in composites than the composites prepared by MM.

The morphology of the cryo-fractured surface of the PA6 composites at a BN loading of 20 wt% which prepared by MM and SM were given in Figure 2(a,b) and Figure 2(c,d), respectively. The SEM observations mentioned above revealed the differences in the morphology and internal microstructure of the composites prepared by two methods from different structure levels. It can be concluded that BN exhibited relatively good dispersion into PA6 phase prepared by SM. This could be attributed to the fact that during solution mixing, the PA6 macromolecules can more sufficiently motion and galleries of BN through the solvation effect of formic acid dispersed more effectively.<sup>28</sup> Moreover, commercially acquired hexagonal bulky BN was sonicated vigorously in formic acid for both dispersion and exfoliation thus can expand the surface-to-volume ratio and reduce the aggregation of BN to homogeneous dispersions which finally enhance the thermal conductivity of polymer-BN composites.<sup>12,32,33</sup> On the contrary, the original BN particles was destroyed to brittle failure and a poor dispersion because of simple mechanical blending prepared by MM.<sup>16</sup>

**Crystallization and Melting Behavior (DSC).** The crystalline structure of PA6 can be influenced by processing methods, thermal conditions, stress, moisture, and additives.<sup>34</sup> It was reported that PA6 has three kinds of crystalline forms which

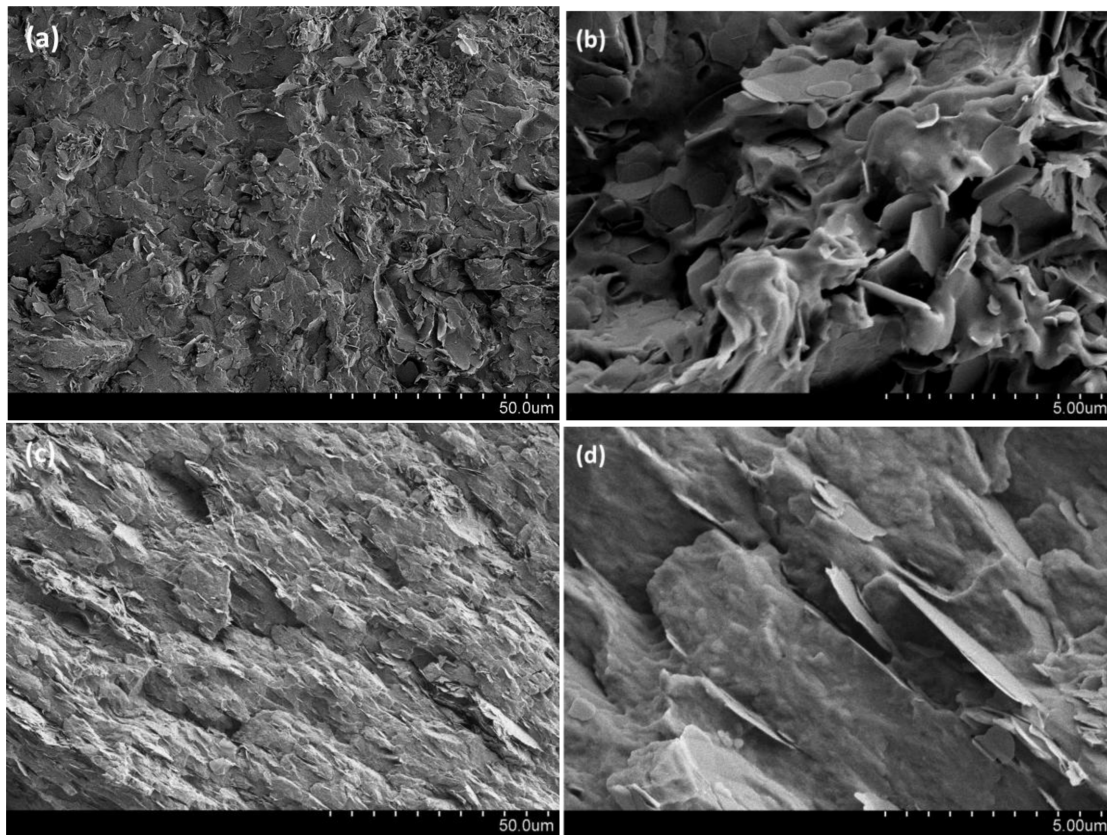


**Figure 2.** SEM images of (a,b) PA6/BN composites prepared by MM; (c,d) PA6/BN composites prepared by SM at a BN loading of 20 wt%.

includes:  $\alpha$ -form,  $\beta$ -form and  $\gamma$ -form.<sup>35</sup> However, it always exhibits two crystalline structures with melting points at 215 °C ( $\gamma$ -form) and 221 °C ( $\alpha$ -form),<sup>36</sup> respectively. For the purpose of comparison, DSC cooling curves and heating curves for neat PA6 and its composites containing various BN contents prepared by MM were shown in Figure 3(a) and Figure 3(b), respectively. The detailed crystallization and melting parameters ( $T_{c,onset}$ : onset crystallization temperature,  $T_c$ : crystallization peak temperature,  $T_{m,onset}$ : onset melting temperature,  $T_m$ : melting peak temperature, and  $X_c$ : crystallinity) were listed in Table 2.

It can be seen that the addition of BN resulted in the increase of onset crystallization temperature ( $T_{c,onset}$ ) and crystallization temperature ( $T_c$ ) as compared with neat PA6. The increase in both onset and peak temperatures might be interpreted as an increase of the rate of the crystallization process, by time-temperature superposition principle. The  $T_{c,onset}$  increased more rapidly than  $T_c$  indicated greater effect on the initial process (i.e., onset of crystallization or “nucleation”) than the process related to  $T_c$  (i.e., the combined process of “nucleation” and “growth” occurring between  $T_{c,onset}$  and  $T_c$ ). This observed difference in the variation of  $T_{c,onset}$  and  $T_c$  with increasing content

**Table 2.** Melting and Crystallization Properties of PA6/BN Composites Prepared by MM

Samples	$T_{c,onset}$ (°C)	$T_c$ (°C)	$T_{m,onset}$ (°C)	$T_{m,1}$ (°C)	$T_{m,2}$ (°C)	$X_c$ (%)
neat PA6	199.96	190.95	198.04	216.03	222.90	30.84
M10	209.26	197.05	198.45	-	220.96	24.23
M20	216.27	197.69	196.65	-	220.90	22.36
M30	217.56	197.84	199.07	-	221.42	22.11
M40	217.42	198.31	198.23	-	221.45	22.16

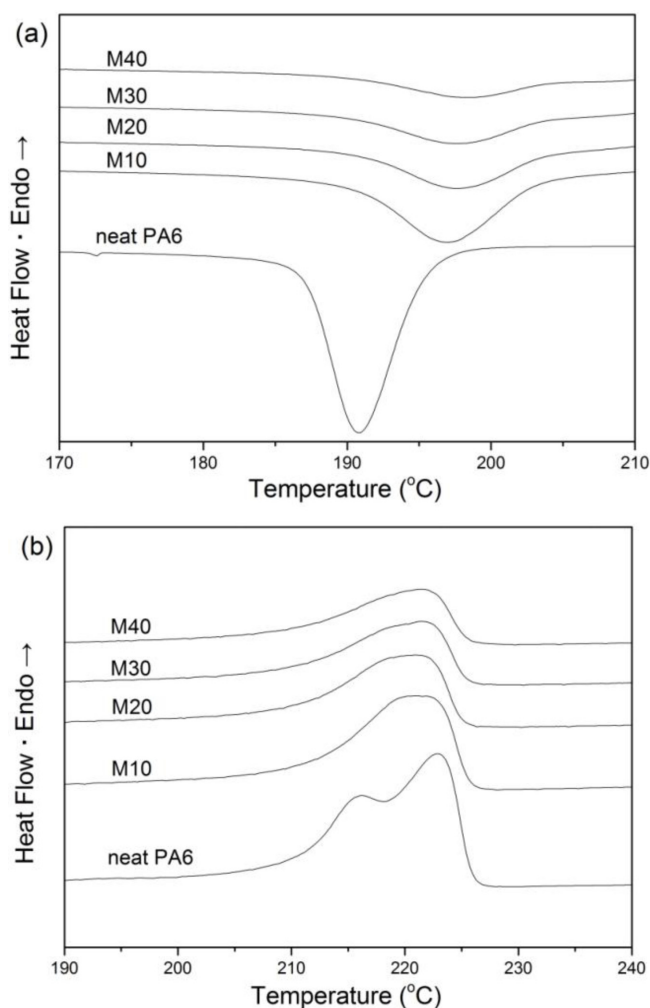


**Figure 3.** DSC curves of PA6/BN composites prepared by MM: (a) cooling curves; (b) heating curves.

of the h-BN filler revealed a role of the filler on crystallization behavior such that the h-BN enhanced nucleation but slowed down growth rate. The slowing down of the growth rate might be attributed to restriction to molecular chain mobility of PA6 caused by the presence of h-BN filler.<sup>37</sup>

It was easy to see that the  $X_c$  of all the composites was lower than that of neat PA6, which indicated that BN filler decreased the crystallization of PA6 matrix. It can be concluded that high BN content would restrict or block the movement and rearrangement of PA6 macromolecular chains, leading to more imperfect crystals and lower crystallinity. The results were similar to the report by S. Şanlı,<sup>38</sup> who pointed out that the crystallinity of PA6 matrix decreased with the addition of inorganic fillers. As shown in Figure 3(b), the heating curve of neat PA6 had two endothermic melting peaks (noted as  $T_{m,1}$  and  $T_{m,2}$

here) at 216.0 °C and 222.9 °C, which were associated with the  $\alpha$ - and  $\gamma$ -form crystals. It can be drawn that neat PA6 showed two common crystals ( $\alpha$ - and  $\gamma$ -form crystals) during the secondary melting process, probably owing to the imperfect  $\alpha$ -form crystal formed during cooling process of the first run.

The  $\alpha$ -phase crystal was a thermodynamically more stable phase, which adopted a fully extended configuration with anti-parallel chains linked by hydrogen bonds to adjacent chains. The  $\gamma$ -phase crystal of PA6 consisted of parallel adjacent chains with hydrogen bonds between them.<sup>39</sup> It is well known that  $\gamma$ -phase, which is less stable or metastable than  $\alpha$ -phase, can be converted to the  $\alpha$ -phase by annealing.<sup>40</sup>

The PA6 composites with different BN loadings showed only one endothermic melting peak, and the only one peak (noted as  $T_{m,2}$  here) tended to move towards a lower temperature and wider. This was probably because that the addition of BN might lead to the mainly formation of  $\alpha$ -form and few  $\gamma$ -form which the former was more thermodynamically stable, and our finding agreed with Fornes *et al.*<sup>41</sup> DSC cooling and heating curves for neat PA6 and its composites with various BN loadings prepared by SM were presented in Figure 4(a) and Figure 4(b), respectively. And Table 3 listed the detailed crystallization and melting parameters. Totally, the effect of BN filler on the crystallization and melting behavior of the composites by SM was consistent with those by MM. For both two processing methods, the temperature of the crystallization peak moved to a higher temperature when compared with neat PA6. The results showed that the h-BN loading had a heterophase nucleation effect on the composites, which seemed to be favorable to the formation of thermodynamically stable  $\alpha$ -phase crystal.<sup>42</sup>

The heating curves of PA6 composites in Figure 4(b) showed one endothermic melting peak as compared with neat PA6. The crystallinity ( $X_c$ ) decreased with increasing BN content as for the composites prepared by SM, but the  $X_c$  values were superior to those of the MM counterparts at the same filler loading. It can be attributed to the reason that hexagonal bulky BN filled in composites was sonicated vigorously in formic acid for both dispersion and exfoliation thus could expand the surface-to-volume ratio, and reduce the aggregation of BN which provided more heterophase nucleation points and increasing the crystallinity of composites.<sup>12,32,43</sup>

In brief, the nucleation mechanism, crystal growth, and final crystal form of PA6 matrix were changed due to the presence of BN filler in the composites.<sup>33,39</sup>

To supplement the DSC observations of crystallization of

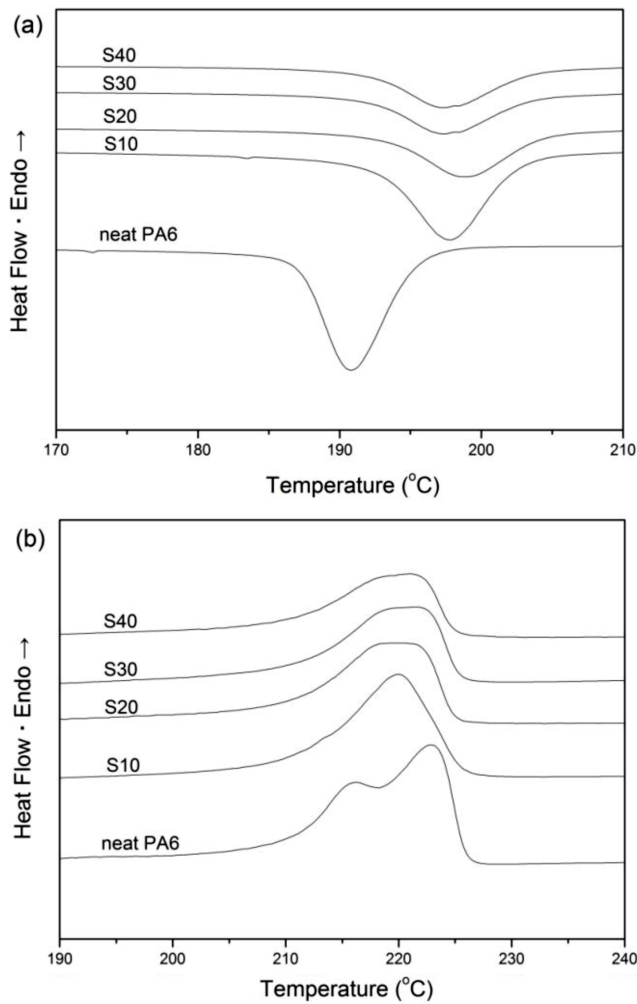


**Figure 4.** DSC curves of PA6/BN composites prepared by SM: (a) cooling curves; (b) heating curves.

PA6 in presence of the h-BN, X-ray diffraction (XRD) investigations were carried out. Figure 5 illustrated the comparison of the XRD patterns of neat PA6, M40 and S40.

The following structural features can be seen: (i) for neat PA6, two main reflections can be observed at about  $2\theta=20^\circ$  and  $23.7^\circ$ , which are attributed to the  $\alpha$ 100 and  $\alpha$ 002/202 crys-

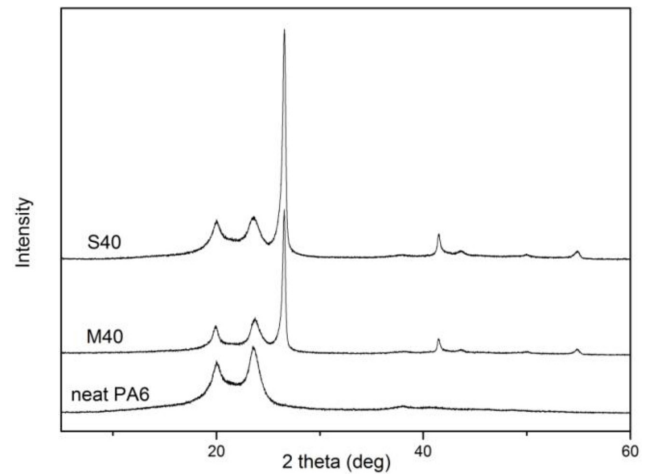


**Figure 5.** XRD patterns of PA6/BN composites prepared by different methods.

tal planes, respectively,<sup>40</sup> implying the absence of  $\gamma$ -form (The reflection peaks at  $2\theta=10.7^\circ$  and  $21.4^\circ$  are associated with  $\gamma$ 020 and  $\gamma$ 001 crystal planes of PA6, respectively.). This supported the possible reason given above for the observed double peaks of the melting endotherm, which means the double peaks in the melting endotherm were due to recrystallization occurring during cooling. (ii) Comparatively, there were only two main reflections can be observed at about  $2\theta=20^\circ$  and  $23.7^\circ$  and some characteristic peaks of boron nitride for the PA6/BN composite. Combined with one peak of the melting endotherm of PA6/BN composite, the addition of BN probably suggested only thermodynamically stable form of  $\alpha$ -phase crystals are induced during heating.<sup>37</sup>

**Thermogravimetric Analysis.** Thermal stability is an essential property of electronic packaging materials and became the limiting factor in both processing and applications which including thermal degradation and thermal aging.<sup>44,45</sup> Thermogravimetric analysis (TGA) can be used as a way to measure the thermal stability and the thermal degradation of polymer due to the simplicity of the weight loss method.<sup>46</sup> There are two kinds of changes in the process of heating: phys-

**Table 3. Melting and Crystallization Properties of PA6/BN Composites Prepared by SM**

Samples	$T_{c,onset}$ (°C)	$T_c$ (°C)	$T_{m,onset}$ (°C)	$T_{m,1}$ (°C)	$T_{m,2}$ (°C)	$X_c$ (%)
neat PA6	199.96	190.95	198.04	216.03	222.90	30.84
S10	206.84	197.84	198.40	-	219.31	26.50
S20	209.69	198.96	197.06	-	219.98	27.47
S30	208.42	197.37	199.43	-	220.98	28.32
S40	210.96	197.20	197.64	-	220.45	28.20

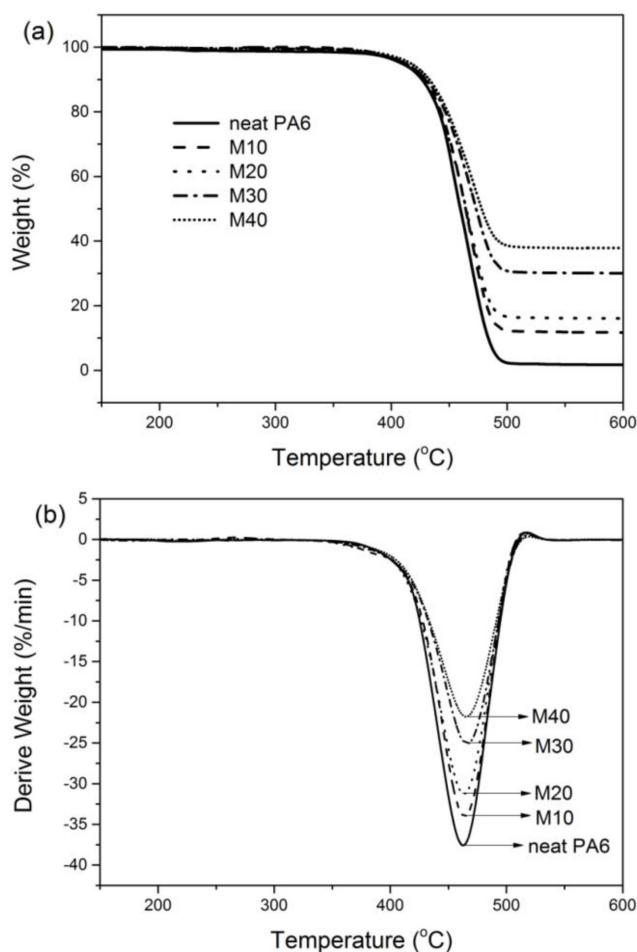


**Figure 6.** TGA curves of PA6/BN composites prepared by MM.

ical changes: softening and melting; chemical changes: cyclization, crosslinking, oxidation, chain scission and degradation. Typical TGA and DTG curves of neat PA6 and PA6/BN composites with different BN loading under nitrogen environments prepared by MM were shown in Figure 6(a) and Figure 6(b), respectively. The detailed TGA data were summarized in Table 4. A sudden drop in the mass of the sample indicated the thermal degradation of the PA6 matrix, and the residual after degradation possibly was BN as the content was similar to the BN loading.

The initial decomposition temperature  $T_{\text{onset}}$  of neat PA6 and M40 had found to be 390.2 and 395.6 °C, respectively. The temperature of maximum decomposition rate ( $T_{\text{max}}$ ) of neat PA6 and M40 were 463.2 and 465.3 °C, the more loading of BN, the higher the degradation temperature was. These results confirmed that the addition of BN increased the degradation temperature and improved the thermal stability of the com-

**Table 4.** TGA Data of the Different BN Contents in PA6/BN Composites Prepared by MM

Samples	$T_{\text{onset}}$	$T_{10\%}$	$T_{\text{max}}$
Neat PA6	390.2	425.4	463.2
M10	392.4	427.8	463.5
M20	392.7	430.3	463.8
M30	393.1	432.3	466.7
M40	395.6	431.0	465.3

posites. But the improvement of the composites' thermal stability were not rarely remarkably. This could be attributed to two reasons,<sup>42,47</sup> on the one hand, the heat absorption capacity and thermal conductivity of BN was higher than that of PA6, which was able to absorb more heat and help heat transfer release. On the other hand, the presence of BN filler might hinder the movement of the molecular chain of PA6, which delayed the maximum decomposition rate of the composites.

The TGA and DTG curves of neat PA6 and PA6/BN composites prepared by SM were given in Figure 7(a) and Figure 7(b), respectively. The detailed TGA parameters were summarized in Table 5. The degradation of PA6/BN composites prepared by SM showed similar trend as MM. But the effect on improving composites' thermal stability were much more obviously than MM. It can be clearly seen that the  $T_{\text{onset}}$  of S40 had reached 412.3 °C (i.e., 22.1 °C higher than that of neat PA6). Compared with neat PA6, the thermal stability of PA6/BN composites prepared by two methods were both enhanced. As the data were observed right before, the composites prepared by SM had better thermal stability compared to the composites prepared by MM, which can be explained by the reason of BN had a better compatibility with PA6 and hindered the movement of PA6 macromolecular chains more seriously.<sup>45</sup>

**Rheological Properties.** For polymer or nanocomposites, rheological measurements are considered to be practical and accurate tool for determining the percolation threshold and also probing microstructural features of the system. The rheological curves of PA6 composites prepared with two methods and measured at 270 °C, including complex viscosity ( $\eta^*$ ) vs. frequency, complex modulus ( $G^*$ ) vs. frequency, and  $\log G''$  vs.  $\log G'$  plots were presented in Figures 8 and 9.

It was clearly appeared that the values of complex viscosity ( $\eta^*$ ) and complex modulus ( $G^*$ ) of the composites at low filler contents were similar to neat PA6. But the more packing content in PA6, the more apparent increase in  $G^*$  and  $\eta^*$ . The complex viscosity ( $\eta^*$ ) increased in the low  $\omega$  region with an

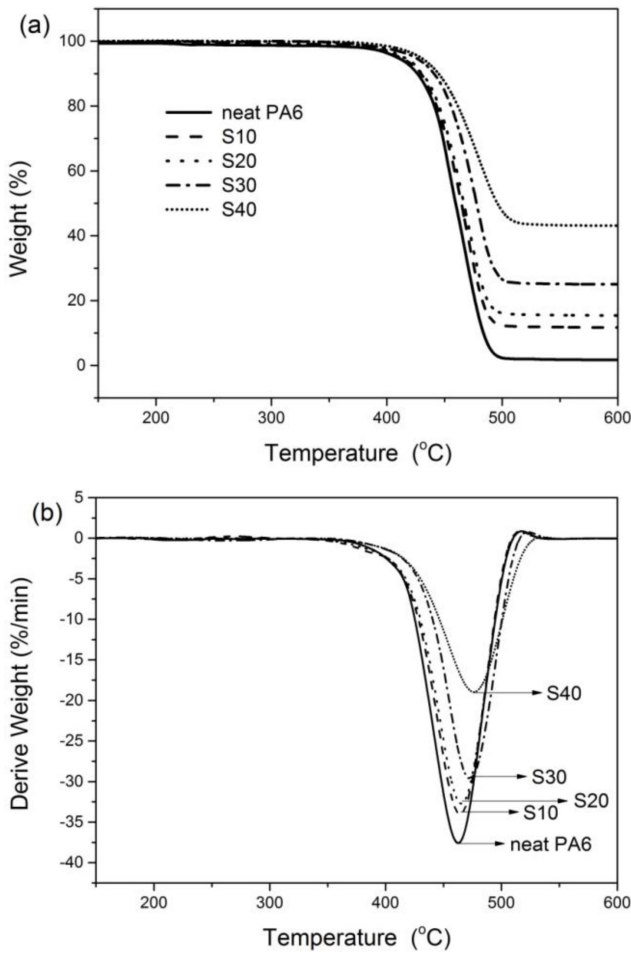


**Figure 7.** TGA curves of PA6/BN composites prepared by SM.

**Table 5.** TGA Data of the Different BN Content in PA6/BN Composites Prepared by SM

Samples	$T_{onset}$	$T_{10\%}$	$T_{max}$
Neat PA6	390.2	425.4	463.2
S10	395.6	427.3	464.3
S20	402.7	430.7	464.8
S30	408.5	440.5	472.5
S40	412.3	443.8	476.1

(unit: °C)

incremental filler content because BN hinders the melt flow of the composites. At the higher frequency region, there was a tendency for the curves to coincide with each other, which was a typical phenomenon of shear-thinning behavior.<sup>48</sup>

Figures 8(c) and 9(c) presented the  $\log G''$ - $\log G'$  plot, which can be used to analyze miscibility and dispersion of filled polymer composites.<sup>49</sup> The curves of composites with low filler contents showed second platform and disappeared at high filler contents, this relationship is a common phenomenon for the

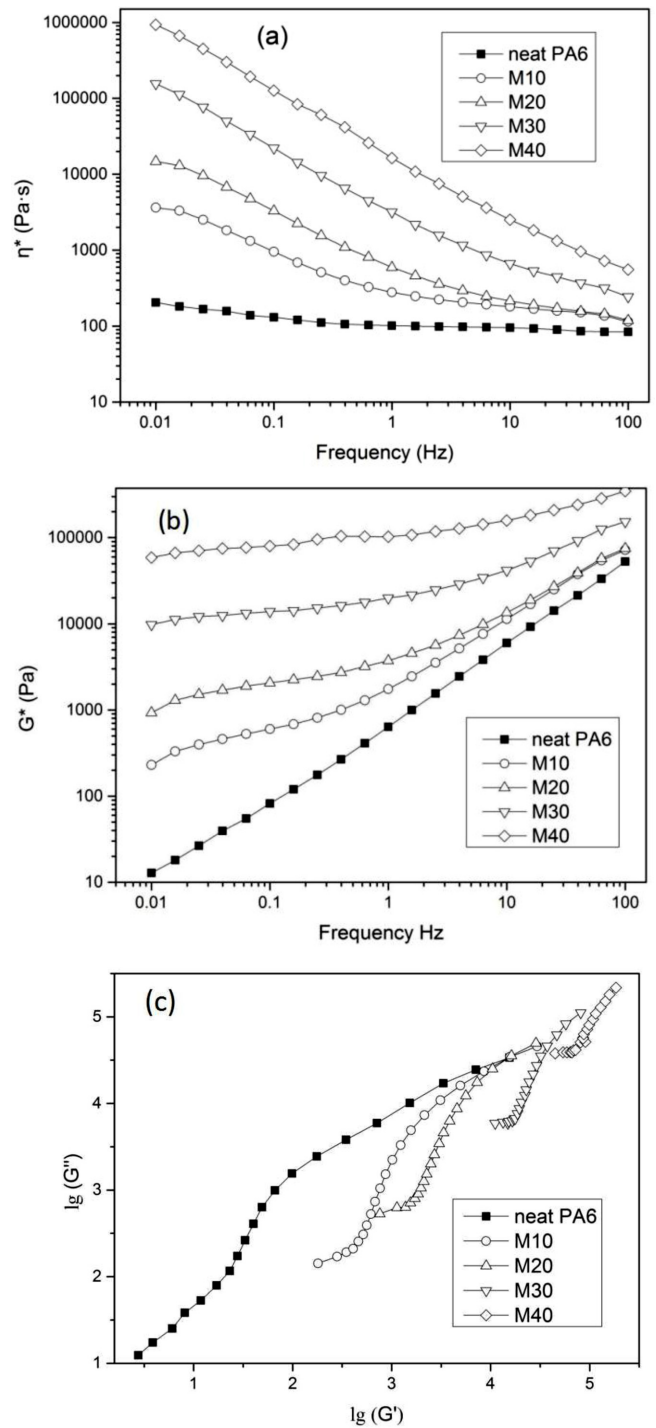


**Figure 8.** Rheological properties of PA6/BN composites prepared by MM with different BN contents under 270 °C as indicated in the graphs: (a) complex viscosity ( $\eta^*$ ) vs. frequency; (b) complex modulus ( $G^*$ ) vs. frequency; (c)  $\log G''$  vs.  $\log G'$ .

composites called pseudo solid-like behavior, which indicated a physical network formation by the inorganic fillers.<sup>50,51</sup>

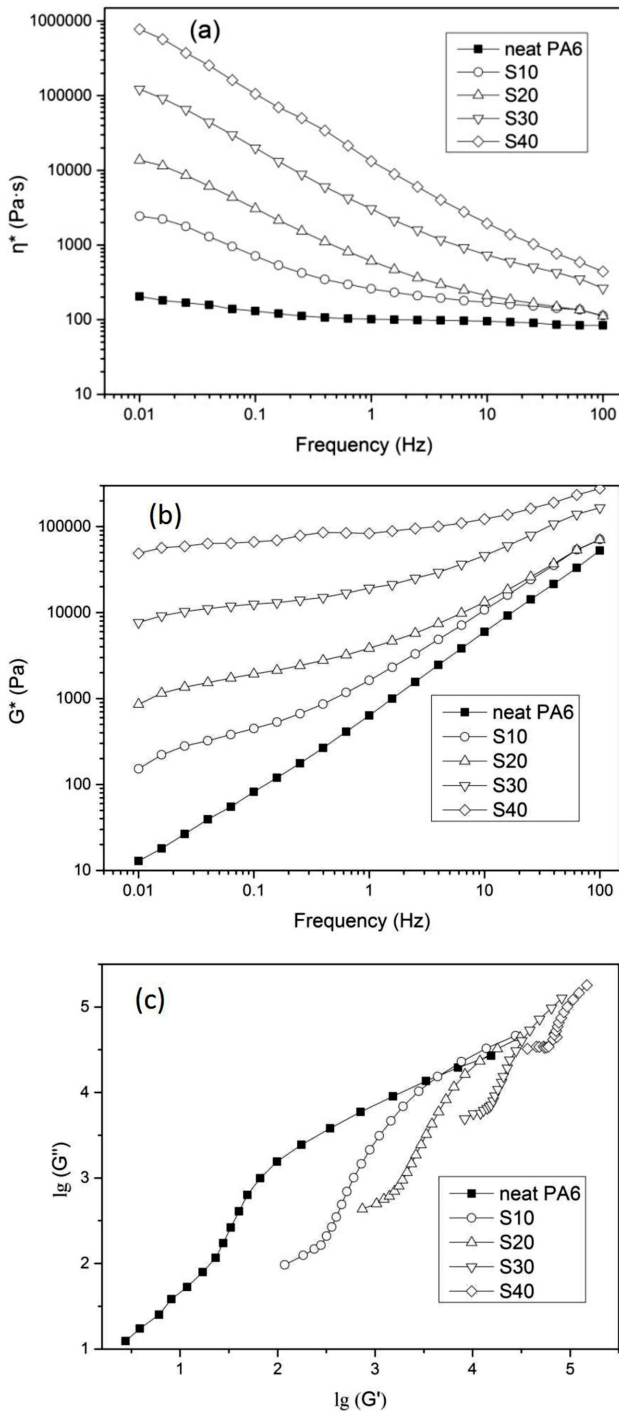


**Figure 9.** Rheological properties of PA6/BN composites prepared by SM with different BN contents under 270 °C as indicated in the graphs: (a) complex viscosity ( $\eta^*$ ) vs. frequency; (b) complex modulus ( $G^*$ ) vs. frequency; (c)  $\log G''$  vs.  $\log G'$ .

In addition, the curves changed to a narrower region with increase in the BN content, which was attributed to the restriction of micromolecular chains and difficulty in forming homo-

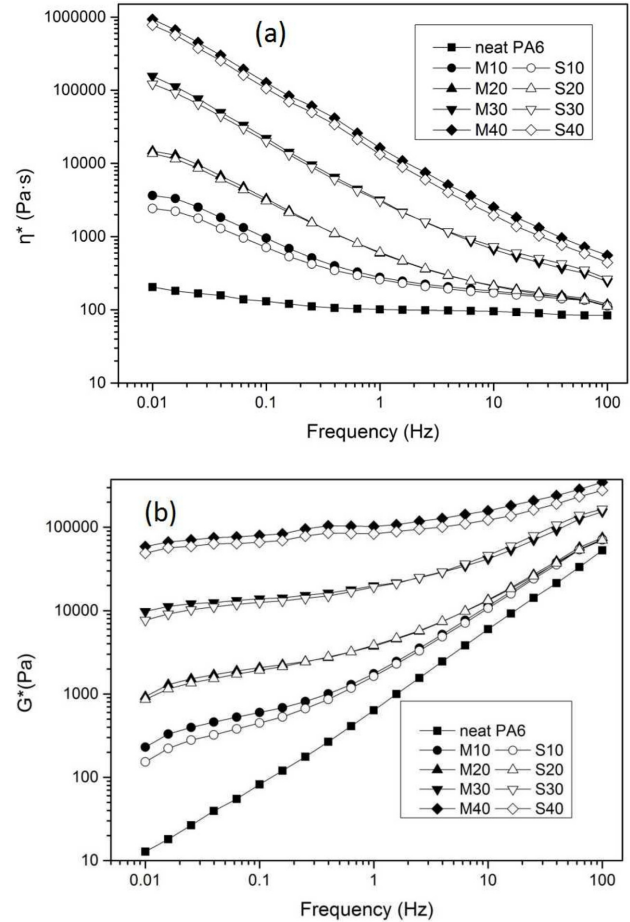


**Figure 10.** Comparison of PA6/BN composites' rheological properties prepared by MM and SM with different BN contents under 270 °C as indicated in the graphs: (a) complex viscosity ( $\eta^*$ ) vs. frequency; (b) complex modulus ( $G^*$ ) vs. frequency.

geneous system at large filler content. And further illustrated there existed immiscible or phase-separated region in polymer composites but two mixing methods obviously different.<sup>50</sup>

As shown in Figure 10, for both series of samples, the modulus of the composites increased with the increasing BN content within the entire frequency range. Meanwhile, it was clearly seen that the  $\eta^*$  values of the composites prepared by SM were lower than those by MM with same BN loading. The thermally conductive network was possibly formed with *ca.* 30 wt% BN loading. That is, the BN loading between 30–40 wt% would favor the heat conduction of the PA6 composites.<sup>17</sup>

## Conclusions

Thermal conductive composites of PA6 filled with different

BN content were obtained by melt blending (MM) and solution blending (SM) processes. The thermal conductivity, morphology, crystallization behavior, thermal stability, and rheological properties of the composites were investigated. It can be concluded that: the addition of BN filler could significantly improve the thermal conductivity of the composites, and the thermal conductivity of SM is superior to MM. Too much amount of BN would restrict or block the movement and arrangement of PA6 molecular chains, leading to more imperfect crystals and lower crystallinity. Furthermore, the crystalline in the composites were preferred to  $\alpha$ -form crystal. But the crystallinity of the composites prepared by SM were higher than MM because of better heterophase nucleation effect. With the increase of BN weight fraction, the thermal stability of polymer composites for both methods were improved, but the effect on SM was much better. According to melt rheology, the presence of BN particles could increase the melt viscosity and modulus of the composites, since fillers affect the movement of macromolecular chains. Further more, the trend of the frequency dependence of melt viscosity and modulus changed significantly at a certain BN loading concentration. And the effect on the composites prepared by SM were marginally.

**Acknowledgement:** The authors are gratefully indebted to the National Natural Science Foundation of China (No. 51403001). In addition, the financial supports from the Institute of High Performance Rubber Materials & Products (Hefei) were also acknowledged.

## References

1. M. Donald and B. Bigg, *Polym. Eng. Sci.*, **17**, 842 (1977).
2. M. C. Vu, G. D. Park, Y. H. Bae, and S. R. Kim, *Polym. Korea*, **40**, 804 (2016).
3. W. Y. Zhou, S. H. Qi, H. Z. Zhao, and N. L. Liu, *Polym. Compos.*, **28**, 23 (2007).
4. T. L. Li and S. L. C. Hsu, *J. Appl. Polym. Sci.*, **121**, 916 (2011).
5. J. U. Ha, J. Hong, M. Kim, J. K. Choi, D. W. Park, and S. E. Shim, *Polym. Korea*, **37**, 722 (2013).
6. D. L. Gaxiola, J. M. Keith, J. A. King, and B. A. Johnson, *J. Appl. Polym. Sci.*, **114**, 3261 (2009).
7. F. Z. Rafique and N. Vasanthan, *J. Phys. Chem. B*, **118**, 9486 (2014).
8. J. A. Heiser, J. A. King, J. P. Konell, and L. L. Sutter, *Polym. Compos.*, **25**, 407 (2004).
9. Y. Yoo, H. L. Lee, S. M. Ha, B. K. Jeon, J. C. Won, and S. G. Lee, *Polym. Int.*, **63**, 151 (2014).
10. Z. Han and A. Fina, *Prog. Polym. Sci.*, **36**, 914 (2011).
11. Z. G. Li, W. J. Wu, H. Chen, Z. H. Zhu, Y. S. Wang, and Y. Zhang, *Rsc. Adv.*, **3**, 6417 (2013).
12. J. Hong, J. Lee, C. K. Hong, and S. E. Shim, *Curr. Appl. Phys.*, **10**, 359 (2010).
13. S. Z. Yu, P. Hing, and X. Hu, *Composites Part A*, **33**, 289 (2002).
14. Y. Agari, A. Ueda, and S. Nagai, *J. Appl. Polym. Sci.*, **42**, 1665 (1991).
15. T. Liu, J. L. Li, X. Z. Wang, Z. H. Deng, X. J. Yu, A. Lu, F. M. Yu, and J. P. He, *J. Thermoplast. Compos. Mater.*, **28**, 32 (2015).
16. Q. H. Mu and S. Y. Feng, *Thermochim. Acta*, **462**, 70 (2007).
17. M. A. L. Manchado, B. Herrero, and M. Arroyo, *Polym. Int.*, **53**, 1766 (2004).
18. S. P. Liu, S. S. Hwang, J. M. Yeh, and C. C. Hung, *Int. Commun. Heat. Mass.*, **38**, 37 (2011).
19. K. C. Yung and H. Liem, *J. Appl. Polym. Sci.*, **106**, 3587 (2007).
20. E. K. Sichel, R. E. Miller, M. S. Abrahams, and C. J. Buiocchi, *Phys. Rev. B. Condens. Matter.*, **13**, 4607 (1976).
21. D. Golberg, Y. Bando, Y. Huang, T. Terao, M. Mitome, C. C. Tang, and C. Y. Zhi, *ACS Nano*, **4**, 2979 (2010).
22. C. Y. Zhi, Y. Bando, C. C. Tang, H. Kuwahara, and D. Golberg, *Adv. Mater.*, **21**, 2889 (2009).
23. J. N. Coleman, M. Lotya, A. O'Neill, S. D. Bergin, P. J. King, U. Khan, K. Young, A. Gaucher, S. De, R. J. Smith, I. V. Shvets, S. K. Arora, G. Stanton, H. Y. Kim, K. Lee, G. T. Kim, G. S. Duesberg, T. Hallam, J. J. Boland, J. J. Wang, J. F. Donegan, J. C. Grunlan, G. Moriarty, A. Shmeliov, R. J. Nicholls, J. M. Perkins, E. M. Grieveson, K. Theuvsissen, D. W. McComb, P. D. Nellist, and V. Nicolosi, *Science*, **42**, 568 (2011).
24. K. Sato, H. Horibe, T. Shirai, Y. Hotta, H. Nakano, H. Nagai, K. Mitsuishi, and K. Watari, *J. Mater. Chem.*, **20**, 2749 (2010).
25. T. Terao, C. Y. Zhi, Y. Bando, M. Mitome, C. C. Tang, and D. Golberg, *J. Phys. Chem. C*, **114**, 4340 (2010).
26. Z. Q. Kuang, Y. L. Chen, Y. L. Lu, L. Liu, S. Hu, S. P. Wen, Y. Y. Mao, and L. Q. Zhang, *Small*, **11**, 1655 (2015).
27. J. P. Hong, S. W. Yoon, T. Hwang, J. S. Oh, S. C. Hong, Y. K. Lee, and J. D. Nam, *Thermochim. Acta*, **537**, 70 (2012).
28. D. W. Chae and B. C. Kim, *Polym. Adv. Technol.*, **16**, 846 (2005).
29. G. W. Lee, M. Park, J. Kim, J. I. Lee, and H. G. Yoo, *Composites Part A*, **37**, 727 (2006).
30. S. Araby, Q. S. Meng, L. Q. Zhang, H. L. Kang, P. Majewski, Y. H. Tang, and J. Ma, *Polymer*, **55**, 201 (2014).
31. S. S. Li, S. H. Qi, N. L. Liu, and P. Cao, *Thermochim. Acta*, **523**, 111 (2011).
32. J. R. Potts, O. Shankar, S. Murali, L. Du, and R. S. Ruoff, *Compos. Sci. Technol.*, **74**, 166 (2013).
33. T. X. Liu, W. C. Tjiu, C. He, S. S. Na, and T. S. Chung, *Polym. Int.*, **53**, 392 (2004).
34. S. Şanlı, A. Durmus, and N. Ercan, *J. Appl. Polym. Sci.*, **125**, E268 (2012).
35. D. M. Lincoln, R. A. Vaia, Z. G. Wang, and B. S. Hsiao, *Polymer*, **42**, 1621 (2001).
36. M. S. Sreekanth, A. S. Panwar, P. Po'tschke, and A. R. Bhattacharyya, *Phys. Chem. Chem. Phys.*, **17**, 9410 (2015).

37. J. M. Augustine, S. N. Maiti, and A. K. Gupta, *J. Appl. Polym. Sci.*, **125**, E478 (2012).
38. S. Şanlı, A. Durmus, and N. Ercan, *J. Mater. Sci.*, **47**, 3052 (2012).
39. B. Z. Wu, Y. Gong, and G. S. Yang, *J. Mater. Sci.*, **46**, 5184 (2011).
40. I. Y. Phang, J. H. Ma, L. Shen, T. X. Liu, and W. D. Zhang, *Polym. Int.*, **55**, 71 (2006).
41. T. D. Fornes and D. R. Paul, *Polymer*, **44**, 3945 (2003).
42. J. C. Liang, Y. Q. Xu, Z. Y. Wei, P. Song, G. Y. Chen, and W. X. Zhang, *J. Therm. Anal. Calorim.*, **115**, 209 (2014).
43. P. P. Zhang, K. Y. Zhu, L. Q. Su, and X. Ru, *Adv. Mater. Res.*, **621**, 31 (2013).
44. S. Ibrahim and M. R. Johan, *Int. J. Electrochem. Sci.*, **7**, 2596 (2012).
45. Z. F. Wang, R. Qi, J. Wang, and S. H. Qi, *Ceram. Int.*, **41**, 13541 (2015).
46. J. S. Oh, J. M. Lee, and W. S. Ahn, *Polym. Korea*, **33**, 435 (2009).
47. D. R. Holmes, C. W. Bunn, and D. J. Smith, *J. Polym. Sci.*, **17**, 159 (1955).
48. A. Kasgoz, D. Akin, and A. Durmus, *Polym. Eng. Sci.*, **52**, 2645 (2012).
49. G. Jiang, H. X. Huang, and Z. K. Chen, *Polym. Plast. Technol. Eng.*, **50**, 1035 (2011).
50. J. P. Song, J. Y. Kim, and S. J. Lee, *Polym. Korea*, **41**, 722 (2017).
51. H. Kim and C. W. Macosko, *Polymer*, **50**, 3797 (2009).